

PROTECTION OF SUBSEA INFRASTRUCTURE
IN ICE ENVIRONMENTS

KENTON P. PIKE



by

© Kentoll p. Pike

This thesis begins with an overview of the offshore new foundland oil and gas industry. While hydrocarbon resources are plentiful, adverse operating conditions and risk of impact from encroaching icebergs leads to challenges in design, project execution and operation. Acceptable risk levels regarding hydrocarbon release to the environment have to be met by providing sufficient protection for vulnerable assets. A discussion on the parameters involved in determining contact risk between the keel of an iceberg and a

For subsea structures, many protection concepts have been considered for application in

selected concept for major field development and production schemes on the Grand

but only require limited subsea infrastructure. Other protection concepts which have

The protection of subsea installations required for subsea tie-back developments via tubular frame protection structures is proposed in the present study. Three different geometric configurations are analyzed. The first configuration consists of a rectangular

structure has a large circular base and a smaller circular top position, with the top and base connected using straight inclined members to give the appearance of a truncated conical

structural response of the frames subjected to ice loading. Primary failure mechanisms during ice-subsea structure interaction are assessed using an energy approach. Design loads are estimated using a simple ice load model accounting for crushing failure of the

Progress in this research area should involve simulation of a wider range of ice contact events. It is suggested that the finite element model be improved toward continuum

substructure modelled using kinematic constraints representing iceberg size and stability

guidance and I aimed during the completion of this project initially. I would also like to express gratitude to Paul Sluckey, Freeman Ralph, and Tony King of C-CORE for

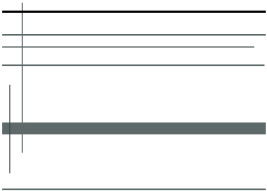
programming knowledge. I thank them both. Also I would like to thank C-CORE for providing me with a space to work, access to software and various reports, and research

questions. MITACS (www.mitacs.ca) granted me an internship scholarship, for that I

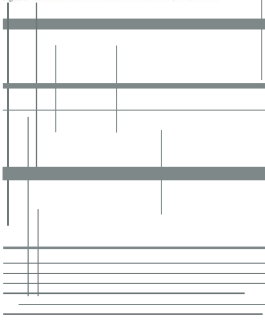
TABLE OF

ABSTRACT.....	
ACKNOWLEDGEMENTS.....	
4 SUBSEA PROTECTION – A REVIEW	29
4.2.6 Caisson Completion System	44
4.2.7 Shear Link Wellhead System.....	46
5.2 Freely-Floating Iceberg Risk	59
5.2.1 Bathymet	
5.2.2 Iceberg frequency	60
5.2.4 Icemax: KcCHCOndizy	63

5.2.5	Iceberg Drift Speed	67
5.3	Scouring Iceberg Risk.....	69
5.3.1	Scour Density	69
5.3.2	Scour Rate	70
5.3.3	Scour Geometry	72
5.3.4	Iceberg Keel Geometry	73
5.4	Calculation of Contact Frequency	74
5.5	Ice Management.....	77
	ICE LOADS.....	80
6.1	Ice-Seabed Interaction Studies.....	84
6.1.1	Rigid Body Kinematic Model	84
6.2	Ice-Structure Interaction Studies.....	85
6.2.1	Initial Kinetic Energy Dissipation Approach.....	85
6.2.2	Continuum Finite Element Analysis.....	88
6.3	Present Investigation - Energy Model for Ice-Subsea Facility Interaction	89
6.4	Present Investigation - Crushing Model	110
	Contact with Rectangular Frame Protection Structure	111
6.4.3	Contact with Truncated Cone Protection Structure	113
	Contact with Truncated Dome Protection Structure	115
7.2	Soil-Pile Interaction	118
7.6	Finite Element Mod ^{el}	129
9	CONCLUSIONS & RECOMMENDATIONS	14
9.1	Ice Loads on Subsea Structures	
9.2	Single-satellite Well Protection Frame Design	



LIST OF FIGURES

- Figure 1- Gullfaks Satellite Tie-Backs (FMC Technologies, 2008).....
Figure 2- Horizontal Tree Dimensions - Back/Front/Side (FMC).....
- 

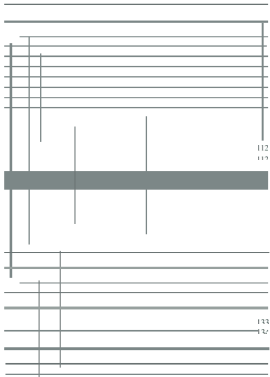


Figure 66- Assumed Undrained Shear Strength Profile (Karlsrud et al., 1993)	155
Figure 67- Horizontal Load versus Lateral Displacement in Clay	156
Figure 68- Depth versus Bending Moment Single Pile in Clay.....	157
Figure 69- Undrained Shear Strength and Shaft Friction versus Depth in Clay.....	158
Figure 70- Axial Pile Head Load versus Pile Head Displacement in Clay	159
Figure 71- Horizontal Load versus Lateral Displacement in Sand.....	160
Figure 72- Depth versus Bending Moment Single Pile in Sand	161
Figure 73- $i-z$ Curve Comparison API versus Measured.....	162

LIST OF SYMBOLS

C_{NET}	Net incremental system cost
C_{CAPEX}	Incremental capex cost
C_{RISK}	Cost of risk from icebergs
	Equipment repair/replacement cost
	Environmental and equipment cleanup cost

H Height of subsea facility above seabed
 D Iceberg draft
 L Waterline length of iceberg

α Annual contact frequency between scouring icebergs and subsea facilities
 β Proportion of icebergs with draft capable of contacting subsea facility

\bar{W}_g	Mean width of free-floating keels
D_f	Effective diameter of subsea facility

Normal force at iceberg keel
Horizontal force at iceberg keel
Vertical force at iceberg keel
Slope angle or structure face

$M_{righting}$ Righting moment of iceberg

\overline{KG}	Distance from keel to center of gravity
I_{sp}	Waterplane moment of inertia
\overline{q}_v	Ultimate vertical bearing resistance of soil

expected to plateau within the next few years meaning new assets need to be exploited to maintain full production capacity. Marginal field development has acted as a catalyst

The present study begins by reviewing the current state of the offshore Newfoundland

production is declining. The issue at the core of this work is the potential for icebergs to

ObjCII impacts or interference from trawl gear. In ice environments the goal is iceberg avoidance or iceberg resistance. For subsea facilities extending above the ocean floor or

containing. The parameters involved in the calculation of risk with free-surface and

The goal of this study is to assess the potential of protecting single salalite oil producing wells using a structural frame. To estimate global loads imposed during the ice keel-

energy to work done through crushing and pitch and heave motions. Based on the analysis, a simplification of the energy model is used. It is assumed conservatively that energy is dissipated in crushing failure of ice over the contact area only

The loads detailed from this approach are then applied to the pre-CCION frame using

developed to simulate pile-soil interaction, soil-structure bearing interaction and global structure response upon application of mean global ice crushing pressures. Three different structural configurations are analyzed and the results are discussed in detail. Finally, conclusions of the present study are drawn and recommendations put forth for

safeguard or single submarine satellite will installations against ice keel contact. The intent is not to propose this idea as the best solution, rather to verify whether or not protection

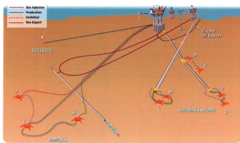
The desired result of the analysis is a nearly optimal protection structure. The first step is

space for ROV access and workover. There should be sufficient clearance to allow

configuration will be made more nearly optimal through successive iterations. The analysis will begin with a simple rectangular frame, similar to conventional protection

inundated cone with straight inclined members. The final design will then take more rounded shapes as the effectiveness of protection frame geometry (i.e. curved versus

Figure 1 depicts Europe's largest fixed-platform subsea-hack development, the



production tree, typically called Christmas (Xmas) tree and wellhead. The Xmas tree comprises valves, spools and fittings with a primary function to direct and control fluid

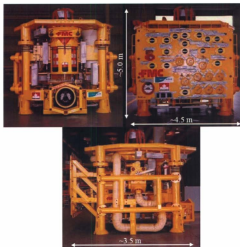
has a relatively low profile height versus the vertical tree leading to a reduction in contact

catastrophic failure modes. In the event of a direct iceberg impact with tree, prevention

production tubing. Stresscs induced in the production tubing, critical to reliable safety valve operation, will likely be higher for a horizontal tree configuration and re-completing

potentially be realized with the implementation of sufficient impact protection

Figure 2 provides approximate dimensions for a typical horizontal tree used offshore

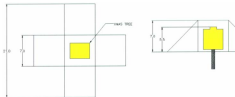


protection structures. Three structural configurations have been conceived based initially

analytical expressions that account for the system energy components and crushing

failure mech _____
modeled usin _____
by piles contr _____
discrete nodal _____
(2000) guide

The global structural responses of a rectangular frame structure (Figure 3) will be compared to that of a truncated cone structure (Figure 4) and then the potential benefit of introducing curved members will be examined as the protection structure takes a dome-like shape (Figure 5). The rectangular frame structure, including pile foundation, has an



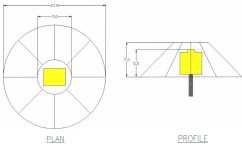
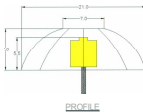


Figure4-Truncated Cone Projection Structure



3 INDUSTRY OUTLOOK

As large offshore discoveries become

economic development of smaller fie

the potential of the West extension has received continued interest (Husky Energy, 2008)

Expansion plans for both the Terra Nova and Hibernia fields also indicate the trend in harnessing the full potential of Newfoundland and Labrador's oil and gas resources. The following figure shows the approximate location of the aforementioned fields with



Figure 6- Offshore Newfoundland and Labrador Oilfields (Rigzone, 2008)

As costs escalate due to strong global demand for services, resources and materials, it is becoming increasingly difficult to make project economics work. The White Rose Southern expansion, for example, adds only a 10% increment to the stated oil reserves but will cost 25% of the original White Rose development budget (The Canadian Press).

province is expected to reach the 400,000 Barrels per Day (BPD) mark with production

expansion of the industry. larger stand-alone field developments or smaller field development with tie-backs to existing infrastructure is required. Park (2007) discussed production trends for the three current producing fields on the Grand Banks: in 2007 a 30 percent decrease in production was predicted by 2011. Without additional development

The majority of oil and gas activity has been focused in the Jeanne D'Arc Basin which is only one of four basins on the Grand Banks with the geological characteristics of oil-bearing rock. All discoveries on the Grand Banks to date have been in this basin while

There are approximately 4 million hectares under license in the offshore areas of

exploration licenses granted for less than a quarter of the total available territory. As a result of three separate bids called by the CNLOPB in 2006, six new exploitation licenses have been granted for six parcels comprising a total of 604,647 hectares. Three of these parcels, which make up approximately 13% of the total area, are located in the Jeanne D'Arc Basin while the remaining area is in the Western Newfoundland and Labrador offshore region (Department of Natural Resources, Gov. NL, 2008). The number of

-
-
- 328 wells had been spudded (spudding is the very start of drilling on a new well).
 - Total industry expenditure was approximately \$21 billion (>1.8 billion on

barrels of natural gas liquids had been discovered (Department of Natural



4 SUBSEA PROTECTION

4.1 Conventional Protection

4.1.1 Protection Frames for:

Protection frames

that there is a large enough risk of accidental loading. Then some means of protection must be provided to protect against these loads. Protection frames apply when there is a risk of dropped object impact loads or snag loads (fishing gear, anchors). Work is currently ongoing for the assessment of protection structures to withstand stronger and

requirements for over-trawlable and dropped object protection structures. Maximum load expected from dropped object impacts and fishing gear are stipulated. For all buildings

is given as 50 kN. A maximum load of 1 MN from trawl ground rope snag is given in the progressive collapse limit state (PLS) for a non-overtrawlable/non-snag-free structure.

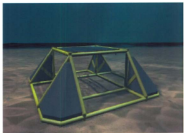


Figure 8-Gravity Subsea Protection (GSP) Frame (Arap Energy, 2(08))

Fail-safe well features play a very important role when evaluating requirements for wellhead protection. Currently, fail-safe systems are adopted as part of the design on every well drilled and perform an important safety function, especially for offshore installations. These safety systems are required to prevent injury to persons, damage to

Subsea completions, which include integral wellhead components, should be designed to

type of fail-safe systems adopted for well installations is the subsurface safety valve

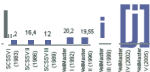
emergency such as a wellhead failure. The safety-valve system is designed to be fail-



Perhaps the most regulated component of an oil and gas well, the SCSSY illustrates satisfy stringent technical, quality and operational requirements. The industry has made huge

reliability. The figure below will illustrate the development in Dappertypc downhole safety

Historical TR-SCSSV (flapper) Reliability



by the Foundation for Scientific and Industrial Research at the Norwegian Institute for Technology (SINTEF) and is currently managed by Wintershall. This study remains the largest yet undertaken into subsurface safety-valve operational experience.

SurCIV valves should be installed at sufficient depth in the production string to maintain integrity as they offer a major risk of environmental damage if compromised. Offshore

in the tubing string at least 30 m below the sea floor, as stipulated by the CNOPB under

An analysis performed by Doha (2007) provides insight into the safe range of depths at which certain downhole components may be set. Significant stresses were found to be nonconservative at typical SCSSV installation levels. Reliance on SCSSV's and other fail-safe systems offers an obvious solution for reduction in overall risk and up-front

ponionofthe Xmas Tree can be placed under a safety class 2 designation as certain components do not contribute greatly to well integrity. This would effectively reduce the

unprotected well in shallower water would be reduced to approximately 9.7×10^{-4} without ice management. These estimates provide motivation for further study of the structural

For an unprotected well, Fowlow (2007) estimates an iceberg contact probability of 9.6×10^{-4} . By refining safety class designations of the Christmas tree, approximately 17% of the tree area can be neglected, achieving a collision probability reduction of 17%. C-

given iceberg contact has occurred, is approximately 0.097. Integrating this suggestion as well as an SCSSV probability of failure of 0.027 an overall blowout probability of 9.7

51.1 years. Fowlow (2007) uses a more conservative value of 36.7, which resulted from

for other potential leak sources. In addition, the dataset may not account for the intended

resulting from iceberg contact and the corresponding effect on SCSSV reliability and

To keep reservoir fluids separate from the environment there are a series of barriers in a well completion. Primary barriers are in full-time direct contact with hydrocarbons while secondary barriers exist as a backup in case of a primary barrier failure and temporary

Doha (2007) performed a fault tree analysis to roughly predict the overall probability of failure of all well integrity components. Failure of production tubing and annulus

tubing hanger and two SCSSV valves. These valves have high reliabilities and their combined effects give a probability of failure of approximately 8×10^{-7} . The annulus barriers - packers, seating joints, tubing hanger seals, and annular isolation valves - give a much greater overall probability of failure of 0.987. The resulting probability of hydrocarbon release to the environment is approximately 0.0127. This fault tree analysis was performed giving the reliability of all potential leak sources equal weight, when in

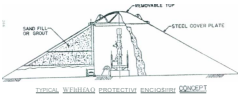


Figure 1]. Protective ShellerConcept (Petroleum Dir(Clorate.Gov.NL.1981)

DORIS Engineering performed a detailed study in 1999 on alternatives to glory holes

protect one to three subsa templates which require a much larger structure than would be required by a single satellite well. Nonetheless, the estimated iceberg loading and necessary structure sideslope would apply. The minimum height was chosen as 10 m

scabed. A horizontal tree, usually around 5m high would require a structure about 8 m high. Figure 2 illustrates the typical protection structure arrangement. A ice crushing strength of 2 MPa was utilized in determining ice loads which ranged from a resultant of

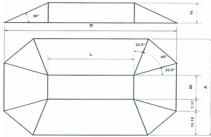


Figure 12- Typical I-Protect structure Arrangement (DorisEngineering, 1999)

The following points briefly outline the various structures considered

sloping face design and external shell of concrete or steel. To be floated and

weight version was considered to reduce installation weight. This version would

separately constructed and transported elements. Similar to the monolithic rigid

- Piled segmental rigid structure; this solution was shown to require a large number of piles to resist the lateral loads and therefore was not investigated further

expected leading to the requirement for a considerable amount of additional

An oil trap pennachthal has been, laminated in the construction of a protective berm around

practicality of this concept is restricted by the extensive amount of sludge material



Boulderscoring icebergs have traversed regions of glory hole installations at depths of up to 15 m in the past (Clark, Hetherington, Zavitz, & O'Neill, 1997). The level of uncertainty and prudence for establishing a conservative design basis will especially safely largely has led recent developments on the Grand Banks, namely White Rose and

Open glory holes originated when drilling activity began in shallow water regions in the

incorporated open glory holes providing about 4 m of scour protection (Carrick, Delong,

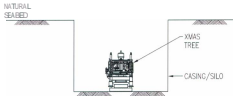
NATURAL
GAS



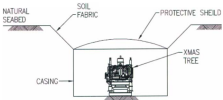
Difficult ground conditions create technical challenges for both the Terra 30va and White Rose glory hole excavations. Cost implications of large open glory holes provide reason to consider ice cheaper alternatives. With an estimated cost of \$9.55 MM CDN (2007), glory holes are not a reasonable iceberg control defense solution for single silos.

typically 6 to 10 meters in diameter and up to 20 m deep. Installation would normally be carried out from a drilling rig. This silo is installed prior to construction of drilling operations. The silo has a weak point at a pre-determined elevation below sea level. In the case of iceberg impact, the silo is sheared at the weak point and the upper part of the silo is sacrificed, leaving the lower part of the silo, the wellhead and the Christmas tree in

A field trial in 1990/10 assess the feasibility of using Tornado Drill technology showed



scgmt by slope excavated sidewalls. Soil reinforcement fabric may be applied to the sloped excavations if necessary to avoid soil slippage. An inner protective shield could also be incorporated to protect the production equipment from debris and make cleanup



multi-well cluster tie-back developments from a risk and cost perspective. The modified cased hole concept was found to be the most attractive option from a combined cost and

assembly consists of all components essential for maintaining wall integrity. The

damage during shear link activation a breakaway flange may be incorporated above the

special running tools and consumable caisson materials are required (Fowlow, 2007)

This concept has been implemented on five exploration wells off the Grand Banks by

as production wells if the fields are found to be commercially viable at later date. As discussed by Fowlow, CFER (1988) investigated the collapse behavior of these 1.067m caisson compliances to assess the effectiveness of the intended protection system. While the relatively unsophisticated analysis yielded favorable results, uncertainties in caisson strength and soil parameters were sufficient to suggest that in SOIIC situations caisson



Figure 7-Caisson Completion Method (Fowlow, 2007)

pipebench at the ocean floor (Ocean Industry, 1978). The above-mudline height was significantly reduced to 4'6" (approximately 1.5m). Master valves and other critical portions of the system are sunk to a required depth and are designed to automatically shut

not including any critical pressure-containing components and in this particular design is covered by a protective dome. New designs (closures) for this concept were prototyped.

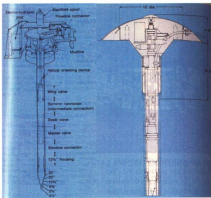
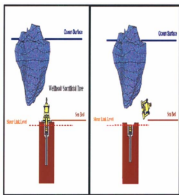


Figure 18-CamcrownworksCaissonCompletionSystem("Ocean Industry,1978)

The concept proposed by Doha (2007) uses off-the-shelf components and can be installed using standard procedures; a convenience feature which would increase attractiveness of any new concept. The difference between this concept and the caisson completion system is the nonrequirement for a lower hanger assembly. Instead, a single isolation ball valve is installed above the tubing hanger. Between the tubing hanger and weak link in the caisson completion system, there consists a lower and upper tree assembly compared



tubing. The intention of the pipe-in-pipe cross section is to decrease stiffness at the shear

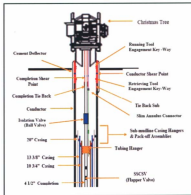


Figure 20-Arrangement of Shear Link Wellhead System (Doha, 2(07)

of this concept is that no special tools, extra excavation or vessel requirement beyond a drilling rig are required for installation of sub-mudline casing and tubing. All

major factor in the relative economic attractiveness of this concept. A downfall of this concept is that while shear links are intended to relieve horizontal loading, they would

not prevent damage from significant vertical forces. The vertical forces created during the interaction process may compress the shear-link disconnect mechanism inhibiting

operation of well integrity components. In a sample calculation, Doha (2007) assumes

in estimating an overall risk level of 1.27×10^{-6} , which is less than the largest safety level of 1×10^{-5} . If we assume ice management is unsuccessful the estimate is increased to

A three year program by GERTH (Groupeement Européen de Recherches Technologiques sur les Hydrocarbures) started in 1976 with the objective of defining and studying the

design of a six-month per-year production scheme as illustrated by Figure 2.1 (see Duval

To place critical components of range of scouring ice keels it was decided to place the equipment on the bottom of a glory hole. The Xmas tree stood at a height of 4 m with a

pull in place to avoid filling by soil cave-ins. Tubing hangers were located in all in caissons approximately 17 m below the excavation bottom. The caisson completion system consisted of a lower tree assembly (slim connector and lower mast valve block) and upper tree assembly (upper fail safe master block, weak point, extension, wye diverter, well vertical access system, flowline connection system). The critical pressure-controlledaining components are located below the weak point. The weak point is incorporated in this particular design as a safety measure in the improbable event of an iceberg keel scouring deep enough to impact the subsea structure. The two hydraulically controlled

This concept includes three separate protection schemes in one: open glory hole, cased glory hole, and caisson completion. For application on the Grand Banks or in any other

design torsurely has had years to develop since this study. The novelty or operating in

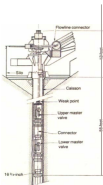


Figure 2 I- Multi-Protection Concept(Duvalet al., 1980)

development in offshore ice environments. An in depth risk analysis is conducted for each concept as well as a detailed nelcostanalysis. Of several novel concepts presented, only the Xmas tree with downhole weak shear plane and the modifiedcaised glory hole

options were deemed worthy of further study due to their favorability from commercial

caisson completion system. A structural based finite element analysis was conducted to predict structural response of a wellhead to iceberg contact. Optimal levels for key components of the completion are suggested. Results of risk analysis based on contact frequency and available reliability data show the potential effects of including downhole

As discussed by Doha (2007), it would still be economically feasible for reservoirs less

protection. A recommendation for new subsurface protection ideas was put forth

Fowlow (2007) performed an in-depth risk and cost study for the various protection concepts. Single well development scenarios as well as multi-well cluster arrangements were analyzed. The annual contact probability was calculated for each concept utilizing

effects of iceberg management with an assumed 85 % effectiveness. From a purely risk based perspective, assuming that ice keel contact results in a well blowout, it was suggested that open glory holes and modified cased glory holes are the most favorable

reduced by shortening the spacing between Xmas trees in the cluster. Fowlow (2007) suggested changing the minimum well spacing from 2.5m to 10 m to reduce contact

The cost of developing an oil field is generally higher offshore than land than in

cost analysis was undertaken for the aforementioned wellhead protection concepts. The net cost of a particular system is evaluated using the following expression

where $C_{\text{net}}^{\text{y}}$ is the net incremental system cost equal to the incremental CAPEX cost (C_{CAPEX}) plus the cost of risk from icebergs (C_{RISK}). Cost of risk can be expressed as

where, θ is the annual probability of iceberg contact, R is equipment repair/replacement cost, E is environmental and equipment cleanup cost, L_g is cost of loss production, and r

singlesatellite well development based on net cost. While an unprofiled well with and

threshold safety limit of 10^{-5} , based on the assumption that iceberg contact causes a well

comparison of the associated costs for each concept. CAPEX has the greatest influence

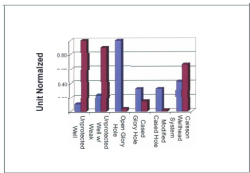
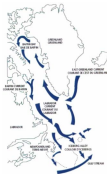


Figure 2.2- Unit Normalized CAPEX & Cost of Risk (Fowlow, 2007)

The majority of icebergs that find their way to the Grand Banks calve off from the West

Icebergs travel north in the West Greenland Current, then south in the Baffin and

2003). Figure 230 outlines the general trajectory of icebergs that may drift in the regions of



icebergs may be freely floating or they may also collide into contact with the seabed causing scours (gouges) or pins. It is worth noting that the Canadian term 'scour' is synonymous with the U.S. term 'gouge'. The number of icebergs which enter the Grand

iceberg season extends from **March** through June. While icebergs are great spectacles for

Acceptable safety or reliability targets associated with subsea installations in ice

offshore codes provide the best design guidance relating to **Grand Banks** ice issues.

	Target Annual Consequences of Failure	Reliability Level
Safety Class 1	Great risk to life or high potential for environmental pollution or damage	1×10^{-5}
Safety Class 2	Small risk to life and low potential for environmental pollution or damage	1×10^{-3}

installation is therefore 1×10^{-5} . Up to about ten entities can be treated individually at this

safety level being maintained at 1×10^{-1} , thereby increasing the safety requirement for each

or injection wells. the environmental impact will be less severe and therefore the safety

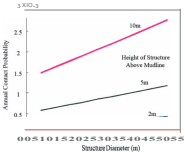
waterline structures separate from the general sea ice load problem. Iceberg loads for

They showed the effect of lowering the vertical profile height of a subsea installation on

between 10^4 and 10^5 which is 100 times higher than a safety class I installation even though a full well blowout is not necessarily a result of impact. A main recommendation from this paper was to assess the risk of structures that protrude above the sea floor by simulation of

To assess iceberg risk to subsea installations which protrude above the mudline we need

to assess the risk of icebergs hitting subsea structures. Figure 24 shows the importance of



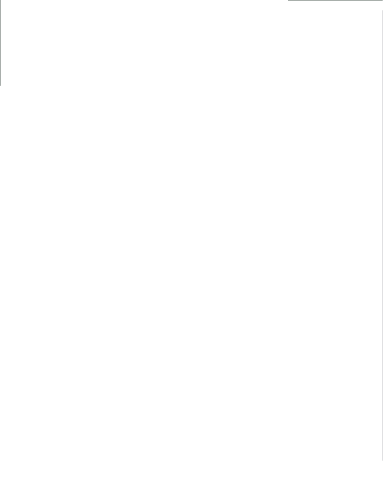
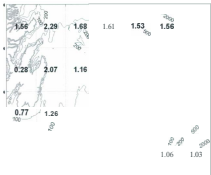


Table 2- Areal Density for Degree Squared Containing Major Developments on the Grand Banks

Time Period	Areal Density (Icebergs/Year/Degree Squared)	Source
1960-2000	0.60	Jordan et al. (1999) in Fowlow (2007)
1981-2000	0.77	Jordan et al. (1999) in Fowlow (2007)
1980-2006	0.79	C-CORE (2007)



In a report by Canence Consultants Ltd. (1999), studies by Brooks (1985), El-Tahan and Davis (1985) and Miller and Holzel (1985) were discussed. Brooks (1985) showed that all iceberg's waterline length is greater than its draft in about 92 % of the cases analyzed.

A scatter plot showing the relationship between draft (d) and waterline length (L_w). The vertical axis is labeled 'd' and ranges from 0 to 4. The horizontal axis is labeled ' L_w ' and ranges from 0 to 2500. Data points are plotted, and a regression line is shown. The equation for the regression line is $y = 0.0001x + 0.77$, where y is L_w and x is d . The correlation coefficient is $R^2 = 0.92$.



$$D = 1.03 \exp(0.70 + 0.78 \ln(L) + E_{\text{rel}})$$

where D is a normally distributed random variable with mean D and standard deviation E_{rel} .

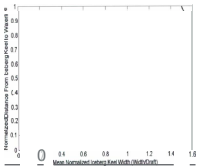
A recent report on ice management (AMEC Earth & Environmental, R.F. McKenna &

Figure 26: Percentage of Free-Floating Kelp Capable of Impact (C-CORE, 2007)

An expression relating normalized icebergwidth (w') to normalizedheightaboveicebergtop (z) is:

$$w' = -9.31z^2 + 5.30z + 0.26$$

known profiles and recommendation is made to incorporate::ucdata from manyicebergs:



Range	Mean Value
100 m > Draft > 90 m	0.22 m/s
105 m > Draft > 85 m	0.24 m/s
110 m > Draft > 80 m	0.30 m/s
Full Region	0.34 m/s
On-shelf	0.32 m/s
Off-shelf	0.35 m/s

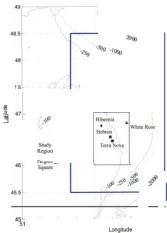
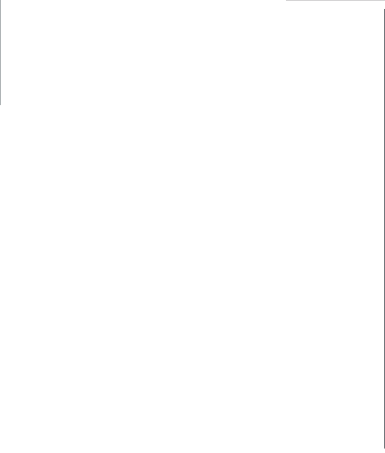


Figure 28-Drift Speed Study Region (Stuckey 2008)

Field specific estimates of mean drift speed should consider the water depth range of the facilities comprising the subsea field layout. It is conservative to use an estimate for the entire study region in the above figure. The following paragraph is a review of other previous estimates of mean drift speed, however, the recent work done by Stuckey (2008)



100,000km²) includes the northeast Grand Banks, Flemish Pass and the westem portion

scour density was 0.56 scours/km² and in depths greater than all 0 m am and is likely or 0.86 scours/km². The variability in local level scour density is noted: there are

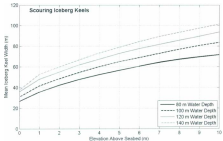
region and mean density of 1.2-1.3 scours/km² between 100-150 m water depth (K.R.

incorporated into the GBSC. A mean scour density of 2.64 scours/km² was determined for the 150 km² region

Scour depths are difficult to measure consistently due to information from various

(Myers & Campbell, 1996) are in close agreement, for water depths ranging from 80-120





through an example pertinent to this study. The theory for this approach was first presented by Sanderson (1988), who developed the method to determine the frequency of

methods requiring estimates of iceberg flux. The following formulae are recently used

where η_0 is the annual average areal density of icebergs, r'_i is the proportion of icebergs with drafts capable of contacting the facility, W_{II} is the mean width of free-floating iceberg keels at the top of the facility, U is the mean iceberg drift speed, and O' is

$$\eta_f = \frac{0.032 \times \left(\frac{0.79 \deg^{-2}}{\cos(49) \times 1.237 \times 10^3} \right) \times 10^{-6} \int_1^{10} (46.67 + 2.1 \times 10^{-3} \times 3.16 \times 10^{-3}) / yr}{= 2.26 \times 10^{-3} \text{ yr}^{-1}}$$

where ρ is the scour rate, L is the mean scour length, W is the mean scouring iceberg keel width at the top of the structure, and O_j is the effective structure diameter

$$\begin{aligned}\eta_0 &= 7 \times 10^{-4} \text{ km}^{-2} \text{ yr}^{-1} \times 10^{-6} \text{ km}^2/\text{m}^2 (72\text{m} + 21\text{m}) \times 650\text{m} \\ &= 4.23 \times 10^{-3}\end{aligned}$$

$$\begin{aligned}\eta &= \eta_f + \eta_i \\ &= 2.26 \times 10^{-3} + 4.23 \times 10^{-3} \\ &= 2.31 \times 10^{-3}\end{aligned}$$

Return periods for contact with each type of approaching iceberg can be determined by taking the inverse of the contact frequencies. The return period for contact with a freely-floating iceberg is approximately 442 years compared with 23633 years for a scouring iceberg. It is clear that freely-floating icebergs dominate contact risk to subssea

The additional comical risk from pinning icebergs (icebergs that create round or oval features on the seabed) will be negligible when compared to the risk from free-floating

Table 5- Input Parameters for Total Contact Probability of a Subsea Facility
Protruding Above the Mudline

	D_f	
Areal Density	η_0	0.79 /degree squared
The Proportion of Icebergs with Drafts Between d_n and d_n+h	r_d	
Effective Keel Width (freely-floating icebergs)	\overline{W}_s	SCCion 5.2.4/Crossdale et al (2000)
Mean Iceberg Drift Speed	\bar{U}	
Annual Scour Rate	ρ_s	
Effective Keel Width (scouring icebergs)	\overline{W}_u	
Mean Scour Length	\bar{L}_s	

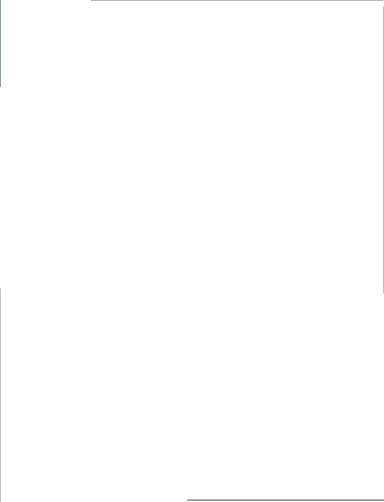
in second place with 5 percent of operations followed by water cannons, nets, and ladders.

In some early reports, has been dismissed due to the associated dangers (Barron et al.,

The following table gives the results of the analysis based on these two definitions of low

Table 6- Ice Management Operational Success (Barron et al., 2005)

Definition	Number of Operations	Percentage of Total
Operational Success	1492	99.1%
Technical Success	1287	85.5%





provides a good fit to empirical data for areas ranging 0.6 m^2 to 6 m^2 . To determine local ice pressures (I_x) corresponding to an exceedance probability (p_x) the following

$$I_x = \alpha \left[-\ln(-\ln(1-p_x)) + \ln \mu \right]$$

where μ can be determined with knowledge of mean event duration / and contact

The term n_p represents the number of events per unit time. Contact frequency - which

(ramming of Kagerøsk vessel, mean duration equals 0.7 s). It is assumed here that each collision qualifies as an event for further detail and explanation see (Jordaen et al., 1993)

pressure-area-secure relationships for calculation of global ice forces. Global ice crushing pressure can be estimated by the pressure-area relationship

$$P = C_P A^{-D_P}$$

where $C_P = 1$ and $D_P = -0.4$ may be taken as mean global values, depending on the application. Jordaen discusses how these results were derived from best fit analysis to ship ram data (Jordaen, 2011). Both C_P and D_P can be taken randomly located the

range of realistic physical situations. The mean is taken in this study as a means of

Parameter	Mean	Standard Deviation	Distribution
C_p	3	1.5	Lognormal
D_p	-0.4	0.2	Normal

It is recognized that high local pressures may exist on smaller areas. Local pressure

curve in Figure 30. Focusing on the 10,000 year local pressure curve it is evident that local pressures at areas greater than around 13 m^2 actually dip below pressures expected globally. At the point where these curves intersect a transition from local to global

mean global pressure calculated for the incremental area in contact. If for example we assume full envelopment of a single tubular member (with a normal projected area of approximately 7 m^2) upon initial contact the area is already close to the local to global

this preliminary analysis. The effects of high local pressures over small contact areas will

procedures may best capture this response mechanism and is a recommended course of

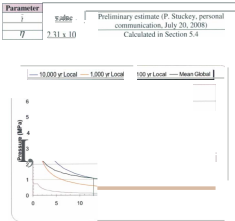


Figure 30- Local Pressure-Area Curves for Varying Return Period & Mean Global Pressure-Area Curve

Iceberg keels scour the seabed when they drift into water depths shallower than their

played a key role in the mode J, which balanced seabed reaction forces, environmental

iceberg hydrostatics is a sensitive parameter in modeling the scour process. Limited

hydrostatics and consequently leads to significant differences in modeled scour lengths

and scouring icebergs were considered. Based on the contact area, a force was calculated from the sampled pressure. Contact areas resulting from free-sailing and scouring icebergs were considered in the analysis. Pressure was assumed to develop uniformly over the entire rigid-body contact area and all impacts were assumed to be direct hits.

with drafts capable of impacting a small ice well 5.5 m in height will pitch sufficiently to allow the keel to pass over the IOP of the structure. For the remainder of the iceberg population, the distance required to dissipate the kinetic energy of the iceberg was calculated based on initial iceberg drift velocity, iceberg mass and impact force applied at

cebe	T	Force (MN)	Moment (MN·m)	Mean	Std.
rg	ype	Mean	Std.	Mean	Std.
Free-noailin		3.3	4.3	9.2	6.6
Scourin		11.9	8.2	18.7	10.3

exceeding 2.8 m^2 to estimate ice keel forces on a thermal protection structures for the

loads ranged from a resultant 40 MN-200 MN on structures which varied greatly in

icebergs with subsea silos would be in the order of 10-30 MN with significant downward

icebergs. The significant downwards forces may have been a result of conservatism in

estimating ice crushing pressures. The coefficient C_1 is taken as 7 and the exponent n is 10.

sacrificial well equipment be located above the seabed and critical equipment be installed

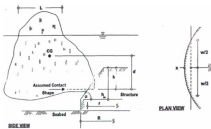


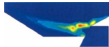
Figure 31-Geometry of Truncated Cone (North Atlantic Offshore Engineering Alliance).

As part of the study, the determination of iceberg loads by energy conservation and momentum conservation approaches was investigated. As well, a numerical model of iceberg motion was accomplished using the discrete element computer package known as

A recent study by Gudmestad and Liferov (2007) assessed ice loads of an ice-ridge keel on a rigid substructure. Two simplified 2D numerical models were developed to

cohesion, keel angle of internal friction). The analysis was performed for shallow, intermediate water depths in ice-covered waters. A sample output graph showed annual exceedance probability versus contact force per meter width for a 10 m wide structure extending 5 m above the mudline in 30 m water depth. It was determined that keel depth or contact height has greatest sensitivity. Possible interaction scenarios were developed

Confined keels, with the high driving forces of the surrounding ice floe were presumed to either shear at the keel, or fail locally and/or globally. Results of the analysis showed that in all but two cases, local propagating failure was the mechanism that limited the keel



The energy approach described herein follows the same procedure outlined in the 1996

relationships had to be modified accordingly; explanation is given throughout this

ice loads imparted on a subsea structure can be estimated using an application of the work-energy principle. Upon impact, the initial kinetic energy of the iceberg will be dissipated through crushing of the ice keel (indentation energy), rotation and heave of the iceberg, and strain energy dissipated by the major load carrying components of the

Energy (2000J). The application of the energy approach in this study does not account for

where $KE_{initial}$ is the initial kinetic energy of the iceberg, E_i is the energy absorbed in sliding (or crushing), E_l the energy initiating the iceberg and E_r inrolling the iceberg

where m is mass, c_a is an added mass coefficient and V is the initial drift speed of the

water surrounding the iceberg. The added mass coefficient can vary between 0.05 for a

extremely high normal forces are generated on contact. Normal and frictional forces can

The moment generated due to the forces at the keel can be calculated by multiplying each force component by its perpendicular distance to the center of gravity of the iceberg.

From the center of gravity of the iceberg, e_x and e_z are the horizontal and vertical

equated to the righting moment to determine the amount of induced rotation. Righting

stability. It is therefore important to integrate stability calculations when considering the

$$M_{righting} = \overline{GM} \sin \theta \cdot \Delta$$

where \overline{GM} is the distance from the center of gravity to the metacenter and Δ is

where V is the submerged or displaced volume. The distance \overline{GM} is given by

where \overline{KB} is the distance from the keel to center of buoyancy. \overline{BM} is the distance from the center of buoyancy to the metacenter line and \overline{KG} is the distance from the keel to

$$M_{\text{righting}} = (\overline{KB} + \overline{BM} - \overline{KG}) \sin \theta \cdot \Delta$$

where I_{cp} is the moment of inertia of the waterplane area, and ∇ is the submerged or displaced volume. Equation 6-15 can then be rearranged as follows

$$\Rightarrow M_{\text{righting}} = \overline{BM} \sin \theta \cdot \Delta - (\overline{KG} - \overline{KB}) \sin \theta \cdot \Delta$$

$$\Rightarrow M_{\text{righting}} = \frac{I_{\text{cp}}}{\nabla} \sin \theta \cdot \Delta - BG \sin \theta \cdot \Delta$$

$$\Rightarrow M_{\text{righting}} = \left(\frac{I_{\text{cp}}}{\nabla} \Delta - \overline{BG} \Delta \right) \sin \theta$$

$$\Rightarrow M_{\text{righting}} = (I_{\text{cp}} \rho_w g - \overline{BG} \Delta) \sin \theta$$

If we assume that for small angles, $\sin \theta \approx \theta$, the expression can be further simplified

an iceberg some angle without performing detailed stability calculations. For an initial

calculate the necessary applied moment at the keel to rotate the ice
estimate of the waterplane moment of inertia. Energy dissipated is
calculated by:

$$\text{Energy} = \frac{\theta}{I_{\text{ice}}} \cdot \omega^2$$

shaped iceberg will be examined. The key parameters from a hydrostatic analysis will be

relative upon initial contact, lessening the amount of energy to be dissipated through crushing of the ice. Energy stored in heaved displacement will in turn add energy to the system in the form of potential energy; the net balance will likely be negligible towards the dissipation of energy. The following paragraphs provide the procedure for

Assuming basic width, side-slope angle (α) and height (h) allows for calculation of the radius of the top area of the truncated cone (refer to Figure 33). With the geometry established, hydrostatics can be used to establish key parameters required to determine the stability of the assumed iceberg shape. To obtain the desired draft, the height can be adjusted and the hydrostatics performed iteratively; the following describes this process.

After selecting a basic radius, side-slope angle and height, the top radius can be calculated by simple trigonometry. The volume of a truncated cone (in this case, the volume of ice)

where h , r_b and r_t are illustrated in Figure 33. The weight of the ice (W_{ice}) which is equal to the buoyant force (FB), can then be calculated by multiplying the volume of ice by the unit weight assuming the density of ice is approximately 925 kg/m^3 .

density of seawater is 1025 kg/m^3

$$V_{water_displaced} = \frac{W_{CG}}{\rho_w g} \quad (\text{Eq. 6-25})$$

required; a solution can be achieved iteratively or using a solver tool such as goal seek in excel. Furthermore, changes to the geometry (i.e. overall height) can be made to achieve the desired draft.

important index of stability at small angles of rotation. Since we are dealing with symmetric geometry in this example, there is no need to distinguish between longitudinal

can be calculated by equation 6-14. The location of the center of gravity for a truncated

$$G = h - \left[\frac{h(r_e^2 + 2r_e r_b + 3r_b^2)}{a(r_e^2 + r_e r_b + r_b^2)} \right]$$

calculated using equation 6-16, where $a = \pi r_e^2$ for a circular waterplane cross sectional area is

After calculating these key parameters, it is relatively simple to calculate the stability curve (GZ curve) for the given shape, taking advantage of the small angle approximation. With sufficient accuracy for all practical purposes the distance GZ can

for a given angle of rotation. Knowing these parameters related to iceberg stability

geometry due to rotation of the iceberg are now accounted for. The normal contact area is

pressure can be approximated by the nominal pressure-area relationship giving normal

will be a sharp increase, and the accumulation of area will continue on linearly thereafter

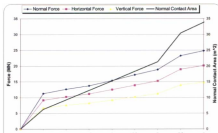
angle of the ship's keel and the coefficient of friction between the keel and structure face.

Figure 34 illustrates the growth of the contact area with horizontal penetration as well as the normal and component forces. The applied moment at the keel is then calculated enabling resolution of the rotation angle. We can also solve for the vertical uplift as the

displacements, the work done by surge, heave and pitch motions will be determined by integration. The cumulative sum of energies after each increment is compared to the

sample calculation is performed for a truncated cone shaped rectangular frame structure as summarized by the parameters

Table 10- Sample Calculation Parameters Trunca



of energies from each contributing mechanism with incremental penetration until all of the energy has been dissipated, as indicated by the % Total Work Done line. From this figure we can see that crushing energy increases rapidly at first due to the fact that the

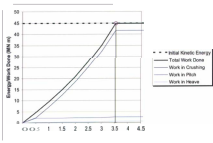


Figure 35. Work Done versus Penetration - Truncated Cone Iceberg Geometry

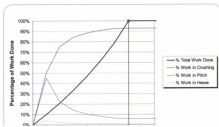


Figure 36- % Work Done versus Penetration-Truncated Cone Icberg Geometry

To establish an upper bound estimate of initial stability, and conversely a lower bound estimate of the energy dissipated through rotation, we can simulate a rectangular prism shape. This presumption is based on the idea that the balance of moments is about the center of gravity will be zero as the horizontal and vertical forces applied at the keel and the moment arms will be practically the same. The calculation procedure is the same as for the previous example, aside from the difference in geometry. The following table

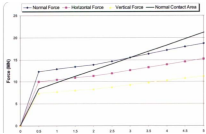


Figure 37. Contact Area & Force versus Penetration - Tabular iceberg Geometry

As can be seen in Figure 39, nearly all of the work is done by crushing of the keel. The

stability in comparison to the previous shape. The other factor which contributes greatly

centerline of the iceberg. The applied moment at the keel about the center of rotation is equal to the horizontal force at the keel multiplied by the distance from the point of

horizontal distance is only a small amount less than the vertical distance, therefore the applied moment at the keel is much lower than for the previous case. From all the results presented in the following two figures, it is clear that the majority of energy is dissipated through crushing before the iceberg comes to rest after surging almost 500

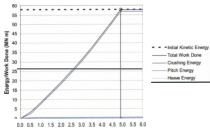


Figure 3S-Work Done versus Penetration for Tabular Iceberg Geometry

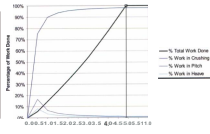


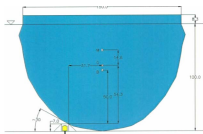
Figure 39- % Work Done versus Penetration - Tabular Iceberg Geometry

The parallel axis theorem for composite sections is used to find G and B . An elliptical

The submerged volume and waterplane moment of inertia are calculated to determine the

than the proportion from pitching. This is likely due to the difference in the slope of the

theoretically came to rest it had pitched about just greater than 0.23° which closely agrees with a mean pitch of 0.24° presented in a similar model used to predict iceberg dynamic



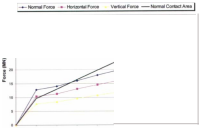


Figure41-Contact Area & Force versus Penetration - Mean Iceberg Geomtry

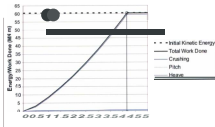


Figure42- WorkDoneversus Penclination- Mean IcebergGeomtry

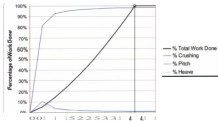
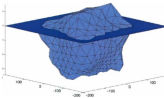


Figure 43- % Work Done versus Penetration - Mean Iceberg Geometry

dissipated entirely through crushing of the keel may be conservative in cases where the initial point of contact is far from the center of rotation of the iceberg. The recommended course of action is to scale existing iceberg profiles of icebergs such that they will have sufficient draft to impact a subsea structure of a given height in a given water depth. For each iceberg, its stability about the varying directions should be determined. Representative contact geometry can be assumed to produce a contact area-penetration

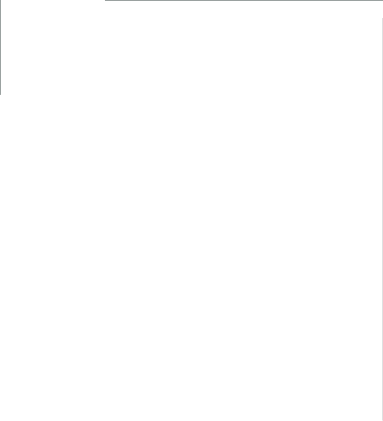
The iceberg in Figure 44 for example will behave differently based on the point of contact. The metacentric height will change about different axes as well as the distance

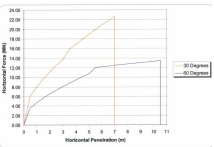
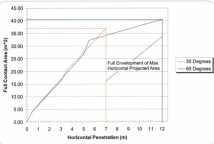
produce very different results with change in the orientation of impact. Application of the Monte Carlo approach is recommended to cover a wide range of iceberg profiles. With



are made to simplify the load transfer process. Scenarios are developed to assess the structural response of a protection frame to loads representative of those that would be imposed during contact with an ice keel. Although a wide range of iceberg load events

the ice-structure interaction process for contact with seabed installations. Based on this assumption, horizontal forces generated by ice crushing pressures and surge penetration will be used conservatively to calculate total work done. Since heave and pitch motions





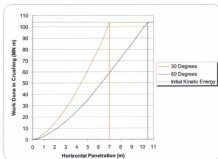
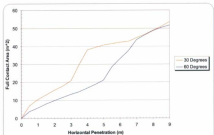
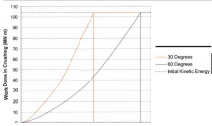
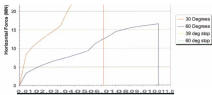
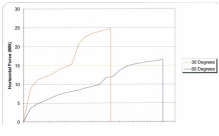


Figure 47- Work Dose in Crushing versus Penetration (Rectangular Frame Structure)

6.4.2 Contact with Truncated Cone Protection Structure







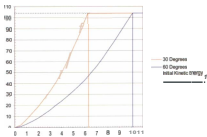


Figure 53 - Work Done in Crushing versus Penetration (Truncated Dome Structure)



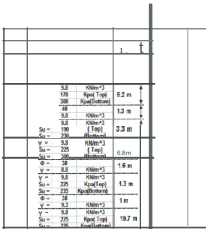
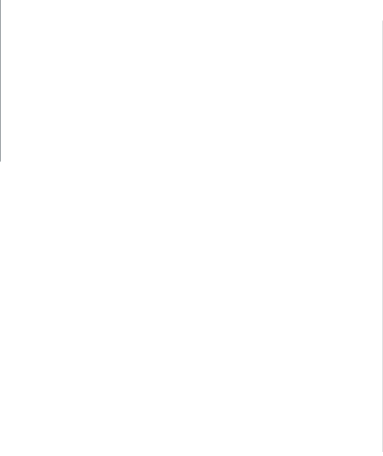
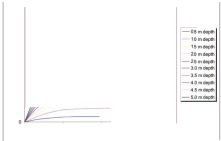
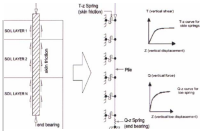


Figure 54-Soil Strength Profile NW Anchor Pile White Rose Field (Doha, 2007)

Each pile connected to the structure is modeled as a separate entity based on the assumption that single-pile load and deflection characteristics will not be affected by adjacent piles. Generally, for piles spacing greater than eight diameters, pile group effects may not have to be evaluated (A.P.L. 2000). Empirical methods, based on model and







where N_s and N_r are bearing capacity factors for vertical strip footings loaded vertically in the downward direction. Y is the effective soil unit weight. r is the total soil resistance per unit length.

$$q_s = cN_s D$$

a relative displacement of approximately $\Delta_{\varphi l} = 0.1D$ for granular soils and $\Delta_{\varphi l} = 0.2D$

$$N_c = [\cot(\phi + 0.001)] \left[\exp[\pi \tan(\phi + 0.001)] \tan^2 \left(45 + \frac{\phi + 0.001}{2} \right) - 1 \right]$$

$$N_q = \exp(\pi \tan \phi) \tan^2 \left(45 + \frac{\phi}{2} \right)$$

$$N_f = e^{0.14(\phi - 25)}$$

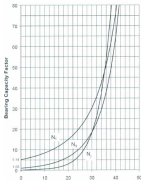
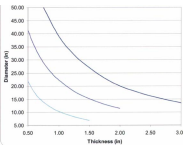


Figure 57- Plotted Values of Vertical Bearing Capacity Factors (American Lifelines Alliance, 2001)

distance of 6 cm and remains constant thereafter. In the present study it is assumed that the

$$M_{\text{applied_max}} = \text{Max} \left[\sqrt{\frac{w}{12}} \left(6Lx - L^2 - 6x^2 \right) \right]$$

$$M_p = \left(1.05 - 0.0015 \frac{D_f}{t} \right) S_{MYS} \cdot D^2 \cdot I$$



Load-displacement relationships for tubular members of offshore structures impacted by

tool for a subsea tubular-frame protection structure thickness formula can be applied. By applying forces resulting from pressures representative of ice crushing strength, we can approximately determine required member sizes to prevent excessive plastic indentation.

where F is the force and δ_p represents the elastic displacement, E is Young's Modulus, γ

length of the contact area along the direction of the tube. The characteristic length is a

discussed by Bai (2003), an empirical equation was obtained through the analysis of linear finite shell element analysis results and indentation tests. A mean value is found to

$$F_0 = 2\sigma_i T^3 L_c / D$$

inclination δ_p can be calculated using a semi-empirical equation. Through energy

unloading point. The local displacement at the load point for a load larger than Pois-

As a simple calculation, we consider a tubular member with a diameter of 0.9m, and thickness

Applying an effective area of $A_e = \pi r^2$ ——————
relationship gives $P = 3 \times 1.54 \times \pi r^2$ ——————
gives a force, $F = 2.34 MPa \times \pi r^2$ ——————
—————

elastic and plastic displacements are $\delta_e = 18.36 \text{ mm}$ and $\delta_p = 24.62 \text{ mm}$. AS 3115 minga

predicts the hardening behavior in the plastic region of the Stress-strain curve (Wikipedia

grades (Walker & Williams, 1995). Figure 59 shows a sample stress-strain curve for x-

	2.55	12.03
-52	2.23	<u>13.67</u>
-56	1.66	17.99
-60	1.48	<u>18.99</u>
-65		25.58
-70	1.13	27.13
	0.86	37.00



modeled using the same elements as for piles (B31). Pipe sections are defined for the

pile and structural member response is based on Timoshenko beam theory assuming

defined by nonlinear spring elements in two transverse directions and the longitudinal

on input parameters (structural dimensions, tubular members size, pile depth and size, and

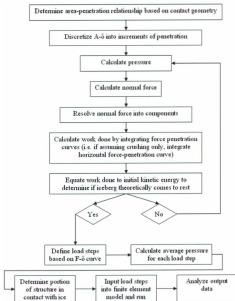
geocell construction) is hence created and tied to the pile foundation. The load application is

approach previously described. The loads are generated in a automated input file generator which creates the input file to be evaluated by ABAQUS/Standard with

and verification through simple structural models. It is recognized that stress intensity

analysis and calibration of the finite element model is recommended

The following flowchart outlines the overall analysis procedure. The main idea is that



This section presents the results of the finite element analyses described in the preceding chapter. There, results are first illustrated for the rectangular frame model. The effect of incorporating curved versus straight members is then shown through comparison of the structural response of the truncated cone and dome models. Based on the outcome of

Note: That the figures provided are scaled to improve visibility of the deformation trends;

undeformed geometries are provided in Section 5. Contact areas are highlighted and

Table4-InputParametersforRectangularFrameGlobalStructural Response Analyses

Parameter	Value	(specified)
ϕ	40°	
γ	8.3325m ⁻¹	

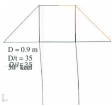
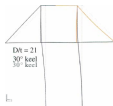
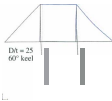
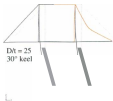


Figure60- Global Structural Response of Rectangular Frame Protection Structure (2.5x magnification)

Soil Parameters	
Pile Thickness	0.050 m
Tubular Diameter	0.6 m (unless otherwise specified)
Soil Type	Sand
ϕ	40°
γ	8.3 kN/m ³

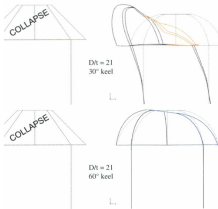
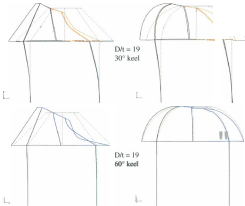


Figure 6 I-Comparison of Truncated Cone and DOME Structures (2.5x)



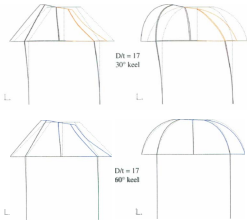


Figure 63-Comparison of Truncated Cone and Dome Structures(2.5x)- Continued

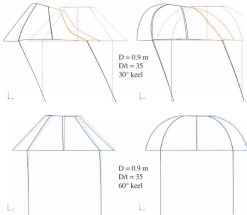


Figure 64-Comparison of Truncated Cone and Dome Structures (2.5x)-C continued

configurations providing increased vertical support for the circular base models could

requirement for the truncated cone and dome geometries. The rectangular configuration

the circular base, adjacent to members under direct pressure, for the other shapes. Since

the side of impact have displaced inwards about 0.9 m. The interaction with the 30° keel

greater vertical component resulting in less horizontal displacement than its counterpart.

Focusing on the frame response with $D/I = 2.5$ in Figure 60, the point of first yield of the

Figure 65. The area between two consecutive vertical lines represents a load step. At this point the ice keel has surged about 3 meters and about 27 % of the assumed initial

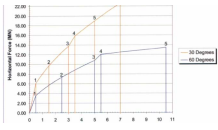


Figure 65- Horizontal Force-Penetration Curve - Load Step Segments

In a side-by-side comparison of the flattened cone and dome models the results shown in Figure 61-Figure 64 consistently demonstrate the improved effectiveness of the dome-like structure in controlling high vertical loads imposed by the 600 keel. Comparison of

Figure 64. The added stiffness sends the forces through the path of least resistance to the

To improve the performance of the truncated cone or dome models it is recommended to

they would likely be more competent in the case of rear-center keel contact

rectangular truss configuration increases its attractiveness. The inclined sections
extending from each side of the interior frame could potentially be constructed and

create unique and extreme challenges in every aspect of new developments large and

A potential solution for the protection of single satellite wells was presented. Three separate configurations were considered under the category of a tubular frame protection

The energy approach was employed with consideration of iceberg stability for simple shapes to assess global loading. The initial kinetic energy of sample icebergs was equalled to the work done in crushing failure of the ice keel over the contact area, and the

simplification of the energy approach which conservatively assumed crushing failure exclusively - in lieu of better understanding - was used to predict loads which were

predicted for each structural configuration and a discussion of the results ensued.

The rectangular frame configurations behaved well under the predicted global loads. The

high vertical pressures without increasing the member size relative to the rectangular frame model; vertical stiffening was recommended. In comparing the truncated cone and

berequiredthatthearea-penetrationsrelationshipbeafunctionofthekelshapeofeachdiscretelysimulatedprofile. Directcentralinteractioneventswithicebergstavelinghorizontallyhavebeenassumedinthe current study. It is recommended to extend loading scenarios to incorporate **non-central** contact which would induce rotation about theverticalaxis. Thepotentialforverticalimpactfroman icebergwillsignificantheave

A potential avenue to capture varying stability and keel geometry is to employ distributions of iceberg metacentricheight (with associated mass and velocity terms) and keel angle. Withkeelangle, thearea-penetrationsrelationship canbeestimatedbasedon contactwithknownstructuregeometry. Fromthearea-penetrationscurve, thecrushingpressurecanbecalculatedfromwhichthenormalforcecanbe calculated and resolved accordingly. The applied horizontal and vertical forces at thekeel determine how much theicebergwillpitchandheavedependingonthestabilityoftheiceberg, which is represented by its metacentricheight. Anmoreaccuratedescriptionof theloadpath during the ice-structure interaction can be achieved by updating the positionofthekeel withrespecttothestructure after each increment of horizontalpenetration

take advantage of the Coupled Lagrangian Eulerian approach being developed in ABAQUS, although the constitutive models for ice would be a significant challenge.

Further work on defining local geometry is recommended to assess the general potential for local protrusions to induce local member failure. In addition to this, the effects of local ice pressures on tubular members should be assessed to further understand potential

Since pile installation on the Grand Banks may be difficult, it may prove beneficial to consider an alternative means to establish adequate lateral resistance. The main downfall

vessel support) and logistics optimization is needed. Once the structural frame

"Ocean Industry," (1978, November). Below mid-Unwell-completenessinsystemsexcellence
iceberg, and/or, break damage. Ocean/Industry. 13(1-2) 64-65

Allen, S. (2000). OTCI 19 E-Global analysis is or wellheads. Selection glory holes for them
nova. *Offshore Technology Conference Proceedings*, Houston, TX, 1-13

ArupEnergy. (2008). Gravity hills ship protection (GSP). Retrieved 04/12/1, 2008, from
<http://www.arup.com/jaccplatforms/downloads/GSP.pdf>

Bai, Y. (2003). *nearShore structures under impact loads. Marville: structural design* (1st ed., pp. 285-304). Kidlington, Oxford, UK: Elsevier Science Ltd

Barron, P., Rudkin, P., Timco, G., & Young, C. (2005). Analysis and i
of iceberg management. Paper presented at the *18th International
Port and Ocean Engineering Under Arctic Conditions, POAC '05*
USA, . 2 595-604. Retrieved from
http://ftp2.crc.nrc.ca/CRTreports/PERD/POAC_05_Towing.pdf

Bass, D. W., & Atwood, D. R. (1986). Iceberg stability - an error and
Science and Technology. 13, 49-55.

C-CORE. (2001a). *Iceberg scour characteristics at white rose* (C-CORE Report No. 00-
C44 Version 2)

C-CORE. (2001 b). *Iceberg loads on a subseawell installation at hibernia* (C-CORE
Report No. ROI -CO I Version 2)

C-CORE. (2001c). *Iceberg loads on a subsea well installation at hibernia - addendum
report* (C-CORE Report No. ROI -CO I (Addendum. Version I))

C-CORE. (2001d). *Iceberg risk to pilJeilles at white rose* (C-CORE Report 0.00-C45
Version 2)

C-CORE. (2007). *Subseafloor risk assessment and mitigation (SIRAM) - state of the art review*(C-COREReportNo.R-06-017-480v2.0)

Center for Frontier Engineering Research (CFER). (1988). *Iceberg collision damage susceptibility of a subsea caisson completion system* (Petro-Canada, Terra Nova Development Studies)

Clark, C., Hetherington, C., Zavitz, J., & O'Neil, C. (1997). *Breaking ice with finesse: Oil & gas exploration in the canadian arctic*. Edmonton, Alberta: Arctic Institute of North America.

Cox, W. R., Reese, L. C., & Grubbs, B. R. (1974). OTC2079 - Field testing of laterally loaded piles in sand. Paper presented at the *Offshore Technology Conference*, Houston, TX.

Crossdale, K., Brown, R., Campbell, P., Crocker, G., Jordaan, I., King, T., et al. (2001). *Iceberg risk to seabed installations on the grand banks*. Paper presented at the *Proceedings 16th International Conference on Port and Ocean Engineering Under Arctic Conditions*, Ottawa, ON, Canada. 1019-1028. Retrieved from ftp://ftp2.crc.nrc.ca/CRTreports/PERD/POAC_01_GB_Scour.pdf

Duval J. J., Mercier, G., & Morin, P. (1980, January). A case of flake oil production from "icebergs-off fested waters". *Icebergs and Oil Pollution*, 5(1), 25-26.

Environment Canada. (2003). Iceberg migration patterns and climatic factors. Retrieved 6/12/2008, 2008, from <http://ice-glaces.ec.gc.ca>

Exprosoft. (2006). Wellmaster (TM): Reliability of well completion equipment. Retrieved 11/12/2008, 2008, from <http://www.exprosoft.com/Products/WellMaster/Web.pdf>

FMC Technologies. (2008). Suloil Hydragulf sank. Retrieved 04/21, 2008, from <http://www.fmc-technologies.com/Suloil/Projects/Norway/S100/KGdEksa.srm>

Fowlow, D. C. (2006). Wellhead protection of ice-prone oil wells. *Journal of Petroleum Technology*, 58(1), 1-8.

Fuglem, M., Muggeridge, K., & Jordaan, I. (1999). Design load calculations for iceberg impacts. *In memory of Olafur Ojarkov and Poul Ellingværslig*, 9(4)

Gahr, M. A., Lunne, T., & Powell, J. J. (1994). P-y analysis of laterally loaded piles in clay using DMT. *Journal of Geotechnical Engineering*, 120(5), 816-837.

Gilbert, D., & Hampton, P. (1990). *Terra nova project studies 1991 hole field trial report* (Terra Nova No. 90-017) Retrieved from ceaa.gc.ca/010/0001/0001/0010/0003/documents_e.htm

GudmCSlad.O.T.. & Lifeson, P. (2007). DesignofsubseacquimentwithStandforces from ice. *Proceedings of POAC-07*. Dalian, China. 787-797

Hanch.S.. & Bai, Y.(2000). Bending moment capacityofpipes. *Journal of Offshore Mechanics and Arctic Engineering*, 122(4),242-253

Internationalice PalooI(IIP). (2008). *What are the sizes and shapes of icebergs?* RCircWd06/25/2008, from <http://www.uscg-millenniarealiip/eagleberga5.shtml>

Jackson, K. (1993, May). Innovation and cost-cutting the keytosuccessasubsea IElectronic versional . *The Oil/mall*, (5)96-98

Jordan, I. J. (2001). Mechanics of ice-structure interaction. *Engineering Fracture Mechanics*, 68(17-18), 1923-1960.

Joendaan, J.J + Press, D., Milford, P.(1999) Iceberg Databases and Verification
PERD/CHC Report 20-41, March, 1999

Lee, M. M. K.,(1999). Strength, stress and fracture analysis so foers horstribular joints
using finite elements. *Journal of Constructional Steel Research*, 51(3), 265-286

Lolk, W. (2006). In Pike K.P. (Ed.). *Re: Directioflollproject -sacrifice; alTreeShear
plate*

-
-
-
-
-
-
-
-
-
-
-
-
-
- PAL. (2001). *The 2001 iceberg season on the grand banks, final report for the grand banks management team*. PAL Environmental Services
- PAL. (2002). *The 2002 iceberg season on the grand banks, final report for the grand banks management team*. PAL Environmental Services
- PAL. (2003). *The 2003 iceberg season on the grand banks, final report for the grand banks management team*. PAL Environmental Services
- PAL. (2004). *The 2004 iceberg season on the grand banks, final report for the grand banks management team*. PAL Environmental Services

Randolph, M.F. (2003). Science and empiricism in principle foundation design
Geotechnique, 53(10), 847-875

Reese, L. C., Cox, W. R., & Koop, F. D. (1974). OTC2080 - Analysis of laterally loaded piles in sand. *Offshore Technology Conference Proceedings*, Houston, TX.

Rigzone (2008). *Map: EastCollisionOffshoreOilfields*. Retrieved October 7, 2008 from http://www.rigzone.com/news/images/datal.asp?img_id=2974

Sanderson, T. J. O. (1988). Ice Mechanics. Risks to Offshore Structures. Graham & Trotman, London.

Standards Norway. (2004). *NORSOK standard N-004 design of steel structures*. Lysaker, Norway: Standards Norway

*WikipediaContributors. (2008). Ramberg-argo/J/relationship. Retrieved 03/29, 2008.
[from https://en.wikipedia.org/w/index.php?title=Ramberg-argo&oldid=198827830](https://en.wikipedia.org/w/index.php?title=Ramberg-argo&oldid=198827830)*

pile thickness was not specified in the available literature, so a D/t ratio of 25 was

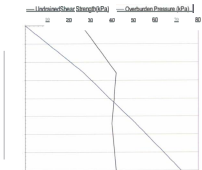


Figure 66-Assumed Undrained Shear Strength Profile (Karlsson et al., 1993)

is approximately 25 %. A comparison or bending moment response for a 20 k¹ load also

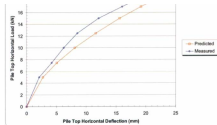


Figure 6-7- Horizontal Load versus Lateral Displacement in Clay

Figure 68-Depth versus Bonding Moment Single Pile in Clay

In a study which examined science and empiricism in foundation design, analytical (2003). As discussed by Randolph, the method of Lardner and Chow known as the MTD diameter pile of 50mm wall thickness. The pile embedment depth was taken as 100m, in clay soil with properties similar to those found offshore W. C. Africa. The effective

unit weight was taken as 3.5 kN/m³ and undrained shear strength (k_s Pa) is approximated

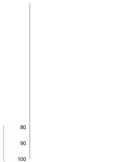
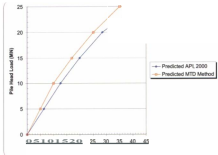


Figure 69 - Undrained Shear Strength and Shaft Friction versus Depth in Clay

displacement obtained from the MTD method and the API guidelines are compared in



embedded to a depth of approximately 2.2 m in sand with an internal angle correction of 39° and an effective unit weight of 10.4 kN/m^3 . The wakertable was maintained above the ground surface during loading to simulate conditions which would exist at an offshore pile, beginning with a load of small magnitude. Groundline displacement and bending

parameters of the field test were matched in the numerical analysis. Results showed good agreement between measured and predicted groundline deflections (see Figure 7.1) with an average error of approximately 16.5 %. A bending moment curve was given in the report for a 266 kN lateral load. Figure 7.2 displays a comparison of the calculated and measured bending moment curve for the 266 kN load. Excellent agreement is achieved

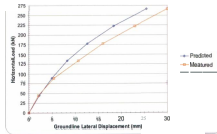
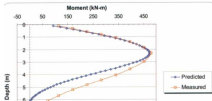


Figure 7.1- Horizontal Load versus Lateral Displacement in Sand



A 1994 study by Al-Shafei et al. involved testing and analysis of tension and compression loads on 0.6 m diameter steel piles driven to 8 m depth in clays and Figure 73 shows a comparison between the idealized bilinear $M-Z$ curve approximated using the API guidelines and the measured $M-Z$ curve from the physical test at 2 m depth.

